HYBRID VOLTAGE REGULATION OF THE NIGERIAN 330 KV GRID USING STATIC SYNCHRONOUS COMPENSATOR AND STATIC SYNCHRONOUS SERIES COMPENSATOR

Akinuli Abimbola Anthony[1] – Akinola Olubunmi Adewale[1] – Adebisi Oluseun Ibrahim[1] – Akinwale Adio Taofiki[2] – Afolabi Segun Akindele[3] – Etinosa Noma-Osaghae[4*]

[1]Department of Electrical and Electronics Engineering, Federal University of Agriculture, Abeokuta, Nigeria
[2]Department of Computer Science, Federal University of Agriculture, Abeokuta, Nigeria
[3]Department of Electrical and Electronics Engineering, University of Ilorin, Ilorin, Nigeria
[4]Department of Electrical and Electronics Engineering, Faculty of Engineering, Olabisi Onabanjo University, Ago-Iwoye, Nigeria

ARTICLE INFO

***Article history*:**
Received: 22.08.2024.
Received in revised form: 07.12.2024.
Accepted: 13.12.2024.

Keywords:
Compensators
Energy savings
Voltage stabilization
Power grid
Power losses

DOI: https://doi.org/10.30765/er.2613

Abstract:

Recently, the control of voltage instability through appropriate power factor correction programmes has become a necessity in power systems due to recurring blackouts and cascading outages that interrupt the smooth supply of electricity to customers. The study examined the combined effect of a Static Synchronous Compensator (STATCOM) and a Static Synchronous Series Compensator (SSSC) for voltage stability enhancement of the Nigerian 330 kV, 28-bus power network. Before compensation, several buses in the network experienced voltage magnitudes below the statutory limit. The application of the combined STATCOM-SSSC system improved the voltage magnitudes at these critical buses, bringing them within acceptable levels. The integration of STATCOM-SSSC also minimized the total active and reactive power losses of the system by 12.51% and 6.65%, respectively, resulting in an annual cost saving of 1.55 billion Naira in power exports. The study demonstrated that the hybrid use of STATCOM and SSSC effectively enhanced the voltage stability of the Nigerian 330 kV power grid. The findings highlight the benefits of implementing advanced reactive power compensation techniques to improve the performance and resilience of the Nigerian power system.

1 Introduction

Reliable and efficient power system operation is a key component in the development of any nation. However, this is only possible if due attention is paid to voltage stability, especially in recent times when power grids have experienced tremendous growth and become increasingly complicated due to the ever-increasing demand for electrical energy as a result of population growth and technological advancement [1][2][3]. Voltage stability is the power system's ability to operate within an acceptable voltage limit regardless of the perturbation imposed on the system in the form of component outage, load increase and other kinds of disturbances [4][5][6][7]. Voltage instability causes the power system to operate inefficiently, and if it is pronounced in the larger sections of the system, it leads to voltage collapse or uncertainty. This condition, it is usually difficult for the voltage to regain recovery [8]. The main source of power system voltage instability is the imbalance between reactive power supply and demand. A power system network possesses a high voltage when it is characterised by surplus reactive power while it has a low voltage when it is deficient in reactive power. Voltage instability or imbalance causes significant problems in the power system including power outages, equipment damage or cascading failures that can jeopardise the successful operation of the overall

* Corresponding author
E-mail address: etinosa.noma-osaghae@oouagoiwoye.edu.ng

system [9] [10] [11]. The instability of voltage, when not adequately, properly and timely addressed, negatively affects the consumers whose lifestyle largely depends on electricity as a key propellant for socio-economic and technological development. Therefore, there is an urgent need to find ways and means to reduce voltage instability by providing adequate compensation for reactive power in the power system.

The prospect of the conventional control techniques including the use of more generators, and capacitor banks as well as the establishment of a new transmission network and upgrade of the existing facilities for power system performance to achieve voltage stability in addition to power loss minimization is hampered by cost, time and environmental factors which are very important to successful implementation of the control measures [12] [13]. This, therefore, creates room for intense research in recent times in the aspect of the utilization of flexible alternating current transmission systems (FACTS) devices such as static synchronous series compensators (SSSC) and static synchronous compensators (STATCOM) for voltage stability improvement in power system for effective and quality service delivery [13]. FACTS devices, apart from being economical and fast-acting for voltage stabilization in power systems; are promising candidates for power flow control, power line transfer capacity improvement and congestion management, enhancement of power system static and dynamic performance, efficient utilization of energy, power factor correction and enhancement of power quality either applied singly or combined [14] [15] [16]. Hence, the interest of this study was to examine the combined effect of STATCOM and SSSC for power system voltage stability enhancement. STATCOM and SSSC respectively belong to shunt and series members of the FACTS family. The application of the two controllers together on a power network will allow the assessment of how the shunt and series compensations offered by the respective devices interact to impact the power system's voltage stability. SSSC and STATCOM are very versatile FACTS compensators that have been deployed in various capacities for voltage instability control in power systems. [17] worked on a comparative evaluation of SSSC and STATCOM for voltage instability and power flow control in a power system network. Simulations were done using MATLAB/Simulink software without and with compensation to determine the system current, voltage, and active and reactive power flows of a two-area, four-machine 11-bus power grid.

The study indicated that SSSC improved the system voltage profile and minimised both active and reactive power losses better than STATCOM on the considered two area network. Improvement of the voltage stability of Ethiopian 400kV, 230kV, and 132kV electricity grids using STATCOM was considered by [7]. MATLAB/power system analysis toolbox (PSAT) was employed for modelling and analysis. Modified voltage stability indices were used to determine the buses that were constrained while particle swarm optimization (PSO) was deployed for optimal location and sizing of the STATCOM. The results obtained from the study showed that the use of STATCOM on the power system network impacted positively on power losses and voltage stability. [18] employed the use of STATCOM for voltage stability improvement subject to various disturbances based on a 5-level diode-clamped converter. The compensation was implemented via finite set-model predictive (FS-MPC) and phase-shifted pulse width modulation (PS-PWM) controllers. Simulations were performed in a Simulink environment and the performances of the controllers were compared. The results from simulations showed that the control methods for actualizing compensation in the network provided significant stabilization of the bus voltages with FS-MPC displaying a better performance in comparison to PS-PWM under the same perturbing actions. Genetic algorithm (GA) based optimal STATCOM siting for power system voltage stability improvement was considered by [19]. Newton-Raphson method was used for the load flow analysis to obtain the system bus voltage magnitudes and phase angles while the optimum point for the STATCOM's siting was identified with GA. The study revealed that optimal siting of STATCOM improved voltage stability and reduced power losses in the power system considered.

The impact of SSSC on the power transfer capability and transmission efficiency of a power network was studied by [20]. The performance of uncompensated and compensated networks was compared considering voltage stability and power losses as criteria. Simulations were done using MATLAB/Simulink software tool. Findings from the work showed that the SSSC application had a significant positive effect on the voltage stability and power flow control on the two grids considered. [21] worked on optimal placement of STACOM for improvement of voltage stability index (VSI) in distributed systems via a PSO. Load flow analysis and the developed PSO-based algorithm for the optimal location of STATCOM were presented. The study established that system VSI, voltage stability and power losses improved significantly with the appropriate STATCOM's placement on the test network. [22] designed a STATCOM and examined its impact on voltage stability and power flow during a three-phase fault occurrence in a power network. The performance of the designed controller was tested on a standard IEEE 5-bus power grid in MATLAB/Simulink environment. The work

showed that the application of STATCOM on the test network did not only improve the system voltage stability but also reduced power losses.

The effect of multi-STATCOM integration on power system voltage stability subject to various loading conditions was considered by [23]. Load factors of 1, 1.5 and 2 were used and simulations were done using the MiPower software environment. The results obtained indicated that STATCOM had a remarkable positive effect on the voltage stability of the system under varying load conditions. [24] proposed the use of STATCOM to tackle voltage instability on the Kenyan electric grid. The grid was modelled and simulated with and without compensation on the power system and it was revealed that the use of STATCOM greatly enhanced the voltage stability on the grid. [25] dealt with optimal STATCOM integration for voltage stabilization and power transfer improvement in a power system network. A GA optimization problem with maximum loadability as the objective function was formulated. The formulated optimization problem was test run on standard IEEE 14-bus and the Indian utility networks. Findings from the research indicated that optimally located STATCOM on both networks, appreciably enhanced voltage stability under different loading conditions with an additional 50% capacity released to meet the active power and loads demand. A thorough assessment of the literature surveyed shows that significant efforts have been channelled towards addressing the voltage instability problems associated with power system network operation using viable solution techniques such as the application of FACTS compensating devices like STATCOM and SSSC which are modern, robust and economical devices. However, voltage instability issues cannot be completely eradicated or eliminated in a power system since different networks may be exposed to a series of different perturbing forces as demand grows persistently, thus, creating a need for continuous voltage stability assessment. Aside from the requirement of continuous assessment and enhancement of voltage stability, the configuration of FACTS controllers that produce the best voltage stability improvement also needs to be continuously assessed to provide information on the right mode of application of these devices to increase their efficiency for the benefit of the overall system. Therefore, going by the reviewed works, extensive investigations which involve the individual analysis of STATCOM and SSSC or comparative evaluation of both controllers have been conducted for power system voltage stability improvement but to the best of the authors' knowledge, attention to the combined used of these devices have not been prioritized as very limited literature are available in this regard [26] [27]. Hence, there is a need to examine the potential of the combined action of these controllers which exist as separate entities in practice. This study aimed to examine the combined effect of SATCOM and SSSC for the improvement of voltage stability in power systems. The power system's steady-state response was modelled through load flow equations. The modelled power system's response with and without three modes of compensation was thereafter carried out. The system voltage profile, power losses, and the cost analysis of the system's real power loss were then determined.

The following are the contributions this study makes to the existing literature:

1. This study examined the effect of the combined use of STATCOM and SSSC on power system performance and provided useful information on the appropriate configuration or connection mode of these devices for power system voltage stability enhancement.
2. This study established that STATCOM and SSSC deployed as a combined controller is a better FACTS compensating device for a power system's network performance improvement than either STATCOM or SSSC as a single controller.

The rest of the article comprises the methodology employed for this study in section II. The results and discussion are handled in section III. The article is then concluded. Recommendations and a reference section are provided at the end of the article.

2 Methodology

Consider an n-bus network which models a typical practical large-scale power system. The complex power (S) supplied from bus i into the network is expressed by equation (1) [28]

$$S_i = V_i I_i^* \tag{1}$$

Where:

$$S_i = P_i + jQ_i \tag{2}$$

$$I_i = \sum_{k=1}^{n} Y_{ik}V_k \; ; i,k = 1,2,\ldots..n \tag{3}$$

with S_i, V_i, I_i, I_i^*, P_i, Q_i, Y_{ik} and V_k as net bus i complex power, bus i voltage, the net bus i current, the complex conjugate of the net bus i current, net bus i active power, net bus i reactive power, transfer admittance between buses i and k and bus k voltage.

The complex conjugate of equation (1) produces equation (4) which decouples into active and reactive power components respectively expressed by equations (5) and (6):

$$P_i - jQ_i = V_i^* I_i = V_i^* \sum_{k=1}^{n} Y_{ik}V_k \tag{4}$$

$$P_i = Re\left\{V_i^* \sum_{k=1}^{n} Y_{ik}V_k\right\} \tag{5}$$

$$Q_i = -Im\left\{V_i^* \sum_{k=1}^{n} Y_{ik}V_k\right\} \tag{6}$$

Expressing V_i, V_i^*, V_k, and Y_{ik} in polar coordinates forms as given by equation (7) in equations (5) and (6) respectively, result in equations (8) and (9) which are together called static power flow equations.

$$\left.\begin{aligned} V_i &= |V_i|e^{j\delta_i} \\ V_i^* &= |V_i|e^{-j\delta_i} \\ V_k &= |V_k|e^{j\delta_k} \\ Y_{ik} &= |Y_{ik}|e^{j\theta_{ik}} \\ e^{j\varphi} &= \cos\varphi + j\sin\varphi \end{aligned}\right\} \tag{7}$$

$$P_i = V_i \sum_{k=1}^{n} Y_{ik}V_k \cos(\theta_{ik} + \delta_k - \delta_i) \tag{8}$$

$$Q_i = -V_i \sum_{k=1}^{n} Y_{ik}V_k \sin(\theta_{ik} + \delta_k - \delta_i) \tag{9}$$

Where θ and δ represent the phase angle differences. Equations (8) and (9) are essential for characterising the power system's steady-state performance. They are non-linear equations whose solutions are obtained via numerical iteration. This study adopted the Newton-Raphson approach because of its fast convergence, accuracy and suitability for large-scale power networks [28]. The resulting linearized set of equations from the application of the Newton-Raphson method to equations (8) and (9) is expressed by equation (10):

$$\begin{bmatrix} \Delta P_2^{(r)} \\ \vdots \\ \Delta P_n^{(r)} \\ \hline \Delta Q_2^{(r)} \\ \vdots \\ \Delta Q_n^{(r)} \end{bmatrix} = \left[\begin{array}{ccc|ccc} \frac{\partial P_2^{(r)}}{\partial \delta_2} & \cdots & \frac{\partial P_2^{(r)}}{\partial \delta_n} & \frac{\partial P_2^{(r)}}{\partial |V_2|} & \cdots & \frac{\partial P_2^{(r)}}{\partial |V_n|} \\ \vdots & \ddots & \vdots & \vdots & \ddots & \vdots \\ \frac{\partial P_n^{(r)}}{\partial \delta_2} & \cdots & \frac{\partial P_n^{(r)}}{\partial \delta_n} & \frac{\partial P_n^{(r)}}{\partial |V_2|} & \cdots & \frac{\partial P_n^{(r)}}{\partial |V_n|} \\ \hline \frac{\partial Q_2^{(r)}}{\partial \delta_2} & \cdots & \frac{\partial Q_2^{(r)}}{\partial \delta_n} & \frac{\partial Q_2^{(r)}}{\partial |V_2|} & \cdots & \frac{\partial Q_2^{(r)}}{\partial |V_n|} \\ \vdots & \ddots & \vdots & \vdots & \ddots & \vdots \\ \frac{\partial Q_n^{(r)}}{\partial \delta_2} & \cdots & \frac{\partial Q_n^{(r)}}{\partial \delta_n} & \frac{\partial Q_n^{(r)}}{\partial |V_2|} & \cdots & \frac{\partial Q_n^{(r)}}{\partial |V_n|} \end{array}\right] \begin{bmatrix} \Delta \delta_2^{(r)} \\ \vdots \\ \Delta \delta_n^{(r)} \\ \hline \Delta \left|V_2^{(r)}\right| \\ \vdots \\ \Delta \left|V_n^{(r)}\right| \end{bmatrix} \tag{10}$$

Where ΔV, Δδ, ΔP and ΔQ give the discrepancy in the voltage, phase angle, active power, and reactive power respectively. The partial derivative components constitute the Jacobian matrix elements. At each iteration level, the discrepancy in active and reactive powers are respectively given by equations (11) and (12) while the new bus voltage phase and magnitude estimates are given by equations (13) and (14) respectively:

$$\Delta P_i^{(r)} = P_i^{sp} - P_i^{(r)} \tag{11}$$

$$\Delta Q_i^{(r)} = Q_i^{sp} - Q_i^{(r)} \tag{12}$$

$$\delta_i^{(r+1)} = \delta_i^{(r)} + \Delta \delta_i^{(r)} \tag{13}$$

$$\left|V_i^{(r+1)}\right| = \left|V_i^{(r)}\right| + \left|\Delta V_i^{(r)}\right| \tag{14}$$

Where r is the iteration count, ΔP_i^r and ΔQ_i^r are active and reactive power discrepancies respectively, P_i^{sp} and Q_i^{sp} denote specified active and reactive powers respectively, P_i^r and Q_i^r are calculated active and reactive powers respectively, $\left|V_i^{(r)}\right|$ and $\delta_i^{(k)}$ denote bus voltage magnitude and phase angle respectively, $\left|V_i^{(r+1)}\right|$ and $\delta_i^{(r+1)}$ denote new bus voltage magnitude and phase angle estimates at iteration $r+1$ and $\left|\Delta V_i^{(r)}\right|$ and $\Delta \delta_i^{(k)}$ bus voltage magnitude and phase angle discrepancies respectively.

The limits of bus voltage magnitude and reactive power are expressed by equations (15) and (16) respectively:

$$V_i^{min} \le V_i \le V_i^{max} \tag{15}$$

$$Q_i^{min} \le Q_i \le Q_i^{max} \tag{16}$$

Where V_i^{min} and V_i^{max} are bus voltage magnitude lower and upper boundaries respectively and Q_i^{min} and Q_i^{max} are reactive power lower and upper boundaries respectively

2.1 STATCOM Power Flow Modeling

Considering that at bus *i* of an n-bus structured power network, STATCOM was installed as a variable generator, the resulting active and reactive powers due to the inclusion of STATCOM are expressed by equations (17) and (18) respectively:

$$P_i = P_i^g + P_i^{STC} - P_i^l \tag{17}$$

$$Q_i = Q_i^g - Q_i^{STC} - Q_i^l \tag{18}$$

Where P_i^{STC} and Q_i^{STC} represent the STATCOM's active and reactive powers, respectively. Equations (17) and (18) are cases of the STATCOM variable generation model. The variable absorption model requires that the P_i^{STC} and Q_i^{STC} signs are interchanged. Considering the basic network model of STATCOM in Figure 1.

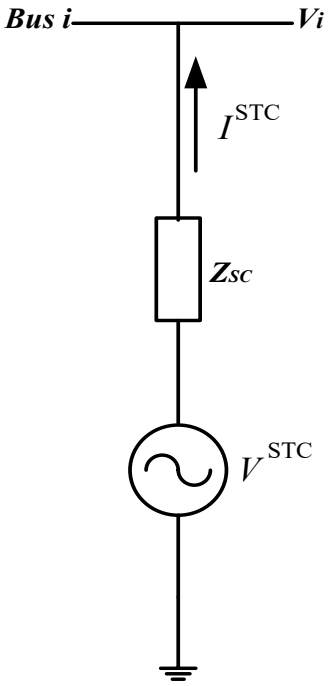

Figure 1. Basic network representation of STATCOM according to Thevenin's theorem [14][29].

The linearized power flow equations for the power system steady-state response modelling are expressed by the matrix of equation (19):

$$\begin{bmatrix} \Delta P_i \\ \Delta|V_i|^2 \\ \Delta P^{STC} \\ \Delta Q^{STC} \end{bmatrix} = \begin{bmatrix} \frac{\partial P_i}{\partial e_i} & \frac{\partial P_i}{\partial f_i} & \frac{\partial P_i}{\partial e^{STC}} & \frac{\partial P_i}{\partial f^{STC}} \\ \frac{\partial |V_i|^2}{\partial e_i} & \frac{\partial |V_i|^2}{\partial f_i} & 0 & 0 \\ \frac{\partial P^{STC}}{\partial e_i} & \frac{\partial P^{STC}}{\partial f_i} & \frac{\partial P^{STC}}{\partial e^{STC}} & \frac{\partial P^{STC}}{\partial f^{STC}} \\ \frac{\partial Q^{STC}}{\partial e_i} & \frac{\partial Q^{STC}}{\partial f_i} & \frac{\partial Q^{STC}}{\partial e^{STC}} & \frac{\partial Q^{STC}}{\partial f^{STC}} \end{bmatrix} \begin{bmatrix} \Delta e_i \\ \Delta f_i \\ \Delta e^{STC} \\ \Delta f^{STC} \end{bmatrix} \tag{19}$$

Where Jacobian matrix elements are defined by equation (20):

Where V^{STC}, I^{STC}, Z_{SC}, I_N and Y_{SC} respectively denote STATCOM voltage, STATCOM current, transformer impedance, Norton's current and short-circuit admittance. S^{STC} is complex power supplied by STATCOM into bus i and I^{STC*}, $V^{STC*}$and Y_{SC}^* are STATCOM current complex conjugate, voltage and short-circuit admittance respectively. e_i and e^{STC} are the real components of the voltage of bus i and STATCOM respectively. f_i and f^{STC} are the reactive components of the voltage of bus i and STATCOM respectively. P^{STC} and Q^{STC} are STATCOM active and reactive power components respectively while G_{SC} and B_{SC} are short-circuit conductance and susceptance respectively [14].

$$\begin{cases} \frac{\partial P_i}{\partial e_i} = G_{SC}(2e_i - e^{STC}) + B_{SC}f^{STC} \\ \frac{\partial P_i}{\partial f_i} = G_{SC}(2f_i - f^{STC}) - B_{SC}f^{STC} \\ \frac{\partial P_i}{\partial e^{STC}} = -G_{SC}e_i - B_{SC}f_i \\ \frac{\partial P_i}{\partial f^{STC}} = -G_{SC}f_i + B_{SC}e_i \\ \frac{\partial |V_i|^2}{\partial e_i} = \frac{e_i}{\sqrt{e_i^2 + f_i^2}} \\ \frac{\partial |V_i|^2}{\partial f_i} = \frac{e_i}{\sqrt{e_i^2 + f_i^2}} \\ \frac{\partial P^{STC}}{\partial e_i} = -G_{SC}e^{STC} - B_{SC}f^{STC} \\ \frac{\partial P^{STC}}{\partial f_i} = -G_{SC}f^{STC} + B_{SC}e^{STC} \\ \frac{\partial P^{STC}}{\partial e^{STC}} = G_{SC}(2e^{STC} - e_i) + B_{SC}f_i \\ \frac{\partial P^{STC}}{\partial f^{STC}} = G_{SC}(2f^{STC} - f_i) - B_{SC}e_i \\ \frac{\partial Q^{STC}}{\partial e_i} = G_{SC}e^{STC} + B_{SC}e^{STC} \\ \frac{\partial Q^{STC}}{\partial f_i} = -G_{SC}f^{STC} + B_{SC}f^{STC} \\ \frac{\partial Q^{STC}}{\partial e^{STC}} = G_{SC}e_i + B_{SC}(e_i - 2e^{STC}) \\ \frac{\partial Q^{STC}}{\partial f^{STC}} = -G_{SC}f_i + B_{SC}(f_i - 2f^{STC}) \end{cases} \quad (20)$$

2.2 SSSC Power Flow Modeling

The Consider a basic circuit of the configuration shown in Figure 2 where the voltage supplied E_{cR} by the compensator and the limits on its magnitude V_{cR} and phase angle δ_{cR} given by equations (21) to (23) respectively [29]:

$$E_{cR} = V_{cR}(\cos\delta_{cR} + j\sin\delta_{cR}) \quad (21)$$

$$V_{cRmin} \leq V_{cR} \leq V_{cRmax} \quad (22)$$

$$0 \leq \delta_{cR} \leq 2\pi \quad (23)$$

The existence of E_{cR} results into two new state variables V_{cR} and δ_{cR} being introduced, thereby leading to the requirement of two new equations for the solution of power flow [29]. The compensator's power flow equations based on the model in Figure 2 are defined by equations (26) to (29) with the Newton-Raphson

linearized version given by the matrix of equation (30):

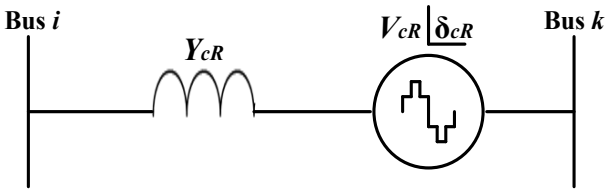

Figure 2. The basic equivalent circuit of SSSC [30].

$$P_{cR} = V_{cR}^2 G_{kk} + V_{cR} V_k [G_{ik} \cos(\delta_{cR} - \delta_i) + B_{ik} \sin(\delta_{cR} - \delta_i)] + V_k V_{cR} [G_{kk} \cos(\delta_{cR} - \delta_k) + B_{kk} \sin(\delta_{cR} - \delta_k)] \quad (24)$$

$$Q_{cR} = -V_{cR}^2 G_{kk} + V_{cR} V_k [G_{ik} \sin(\delta_{cR} - \delta_i) + B_{ik} \cos(\delta_{cR} - \delta_i)] + V_k V_{cR} [G_{kk} \sin(\delta_{cR} - \delta_k) + B_{kk} \cos(\delta_{cR} - \delta_k)] \quad (25)$$

$$P_i = V_i^2 G_{ii} + V_i V_k [G_{ik} \cos(\delta_i - \delta_k) + B_{ik} \sin(\delta_i - \delta_k)] + V_i V_{cR} [G_{ik} \cos(\delta_i - \delta_{CR}) + B_{ik} \sin(\delta_i - \delta_{CR})] \quad (26)$$

$$Q_i = -V_i^2 B_{ii} + V_i V_k [G_{ik} \sin(\delta_i - \delta_k) + B_{ik} \cos(\delta_i - \delta_k)] + V_i V_{cR} [G_{ik} \sin(\delta_i - \delta_{CR}) + B_{ik} \cos(\delta_i - \delta_{CR})] \quad (27)$$

$$\begin{bmatrix} \Delta P_i \\ \Delta P_k \\ \Delta Q_i \\ \Delta Q_k \\ \Delta P_{ik} \\ \Delta Q_{ik} \end{bmatrix}^r = \begin{bmatrix} \frac{\partial P_i}{\partial \delta_i} & \frac{\partial P_i}{\partial \delta_k} & \frac{\partial P_i}{\partial V_i} V_i & \frac{\partial P_i}{\partial V_k} V_k & \frac{\partial P_i}{\partial \delta_{CR}} & \frac{\partial P_i}{\partial V_{CR}} V_{CR} \\ \frac{\partial P_k}{\partial \delta_i} & \frac{\partial P_k}{\partial \delta_k} & \frac{\partial P_k}{\partial V_i} V_i & \frac{\partial P_k}{\partial V_k} V_k & \frac{\partial P_k}{\partial \delta_{CR}} & \frac{\partial P_i}{\partial V_{CR}} V_{CR} \\ \frac{\partial Q_i}{\partial \delta_i} & \frac{\partial Q_i}{\partial \delta_k} & \frac{\partial Q_i}{\partial V_i} V_i & \frac{\partial Q_i}{\partial V_k} V_k & \frac{\partial Q_i}{\partial \delta_{CR}} & \frac{\partial Q_i}{\partial V_{CR}} V_{CR} \\ \frac{\partial Q_k}{\partial \delta_i} & \frac{\partial Q_k}{\partial \delta_k} & \frac{\partial Q_k}{\partial V_i} V_i & \frac{\partial Q_k}{\partial V_k} V_k & \frac{\partial Q_k}{\partial \delta_{CR}} & \frac{\partial Q_k}{\partial V_{CR}} V_{CR} \\ \frac{\partial P_{ik}}{\partial \delta_i} & \frac{\partial P_{ik}}{\partial \delta_k} & \frac{\partial P_{ik}}{\partial V_i} V_i & \frac{\partial P_{ik}}{\partial V_k} V_k & \frac{\partial P_{ik}}{\partial \delta_{CR}} & \frac{\partial P_{ik}}{\partial V_{CR}} V_{CR} \\ \frac{\partial Q_{ik}}{\partial \delta_i} & \frac{\partial Q_{ik}}{\partial \delta_k} & \frac{\partial Q_{ik}}{\partial V_i} V_i & \frac{\partial Q_{ik}}{\partial V_k} V_k & \frac{\partial Q_{ik}}{\partial \delta_{CR}} & \frac{\partial Q_{ik}}{\partial V_{CR}} V_{CR} \end{bmatrix}^r \begin{bmatrix} \Delta \delta_i \\ \Delta \delta_k \\ \frac{\Delta V_i}{V_i} \\ \frac{\Delta V_k}{V_k} \\ \Delta \delta_{CR} \\ \frac{\Delta V_{CR}}{V_{CR}} \end{bmatrix}^r \quad (28)$$

The Jacobian matrix elements are defined by equations (31), the partial derivatives for P_{ik} and Q_{ik} in a similar way as P_i and Q_i.

$$
\begin{cases}
\dfrac{\partial P_i}{\partial \delta_i} = V_i V_k[B_{ik}\cos(\delta_i - \delta_k) - G_{ik}\sin(\delta_i - \delta_k)] \\
\quad + V_i V_{cR}[B_{ik}\cos(\delta_i - \delta_{CR}) - G_{ik}\sin(\delta_i - \delta_{CR})] \\
\dfrac{\partial P_i}{\partial \delta_k} = V_i V_k[-B_{ik}\cos(\delta_i - \delta_k) + G_{ik}\sin(\delta_i - \delta_k)] \\
\dfrac{\partial P_i}{\partial \delta_k} = V_i V_k[-B_{ik}\cos(\delta_i - \delta_k) + G_{ik}\sin(\delta_i - \delta_k)] \\
\dfrac{\partial P_i}{\partial V_i} = 2V_i G_{ii} + V_k[G_{ik}\cos(\delta_i - \delta_k) + B_{ik}\sin(\delta_i - \delta_k)] \\
\quad + V_{cR}[G_{ik}\cos(\delta_i - \delta_{CR}) + B_{ik}\sin(\delta_i - \delta_{CR})] \\
\dfrac{\partial P_i}{\partial V_k} = V_i[G_{ik}\cos(\delta_i - \delta_k) + B_{ik}\sin(\delta_i - \delta_k)] \\
\dfrac{\partial P_i}{\partial \delta_{CR}} = V_i V_{cR}[-B_{ik}\cos(\delta_i - \delta_{CR}) + G_{ik}\sin(\delta_i - \delta_{CR})] \\
\dfrac{\partial P_i}{\partial V_{CR}} = V_i[G_{ik}\cos(\delta_i - \delta_{CR}) + B_{ik}\sin(\delta_i - \delta_{CR})] \\
\dfrac{\partial Q_i}{\partial \delta_k} = V_i V_k[B_{ik}\sin(\delta_i - \delta_k) - G_{ik}\cos(\delta_i - \delta_k)] \\
\dfrac{\partial Q_i}{\partial V_i} = -2V_i B_{ii} + V_k[G_{ik}\sin(\delta_i - \delta_k) + B_{ik}\cos(\delta_i - \delta_k)] \\
\quad + V_{cR}[G_{ik}\sin(\delta_i - \delta_{CR}) + B_{ik}\cos(\delta_i - \delta_{CR})] \\
\dfrac{\partial Q_k}{\partial V_k} = V_i[G_{ik}\sin(\delta_i - \delta_k) + B_{ik}\cos(\delta_i - \delta_k)] \\
\dfrac{\partial Q_i}{\partial \delta_{CR}} = V_i V_{cR}[B_{ik}\sin(\delta_i - \delta_{CR}) - G_{ik}\cos(\delta_i - \delta_{CR})] \\
\dfrac{\partial Q_k}{\partial V_{CR}} = V_i[G_{ik}\sin(\delta_i - \delta_{CR}) + B_{ik}\cos(\delta_i - \delta_{CR})]
\end{cases}
\tag{29}
$$

2.3 The Case Study

The Nigerian 330 kV, 28-bus electricity network was considered to examine the compensating capability of the combined effect of STATCOM and SSSC for voltage stability improvement in this study. The system whose one-line diagram is delineated in Figure 3 and data presented in Tables 1 to 3 comprises twenty-eight buses, fifty-two transmission lines and nine generating stations.

2.4 The MATLAB/PSAT Simulation Environment

The MATLAB/PSAT tool was the simulation environment for this study. PSAT is an open-source software tool that is compatible with MATLAB compatible. It has different useful features including small signal stability optimal power flow, phasor measurement and time domain simulations. PSAT functions can be accessed through a graphical user interface and has a user-friendly Simulink-based library which makes it very suitable for network design and analysis. Therefore, the choice of PSAT for this study.

2.5 The Cost Analysis of the System's Active Power Loss

The cost implication of the losses and savings resulting from the application of the compensators were estimated using the current charge stipulated by the multi-year tariff order of the Transmission Company of Nigeria (TCN) as of 2022. According to TCN (2022), an export of one kilowatt-hour (kWh) energy on the Nigerian electricity grid attracts a basic transmission and administration cost of ₦6.20 and with Nigerian inflation rate of 20.77%, the electric power transmission cost amount to ₦7.49 per kWh. Therefore, the following cost analysis was made:

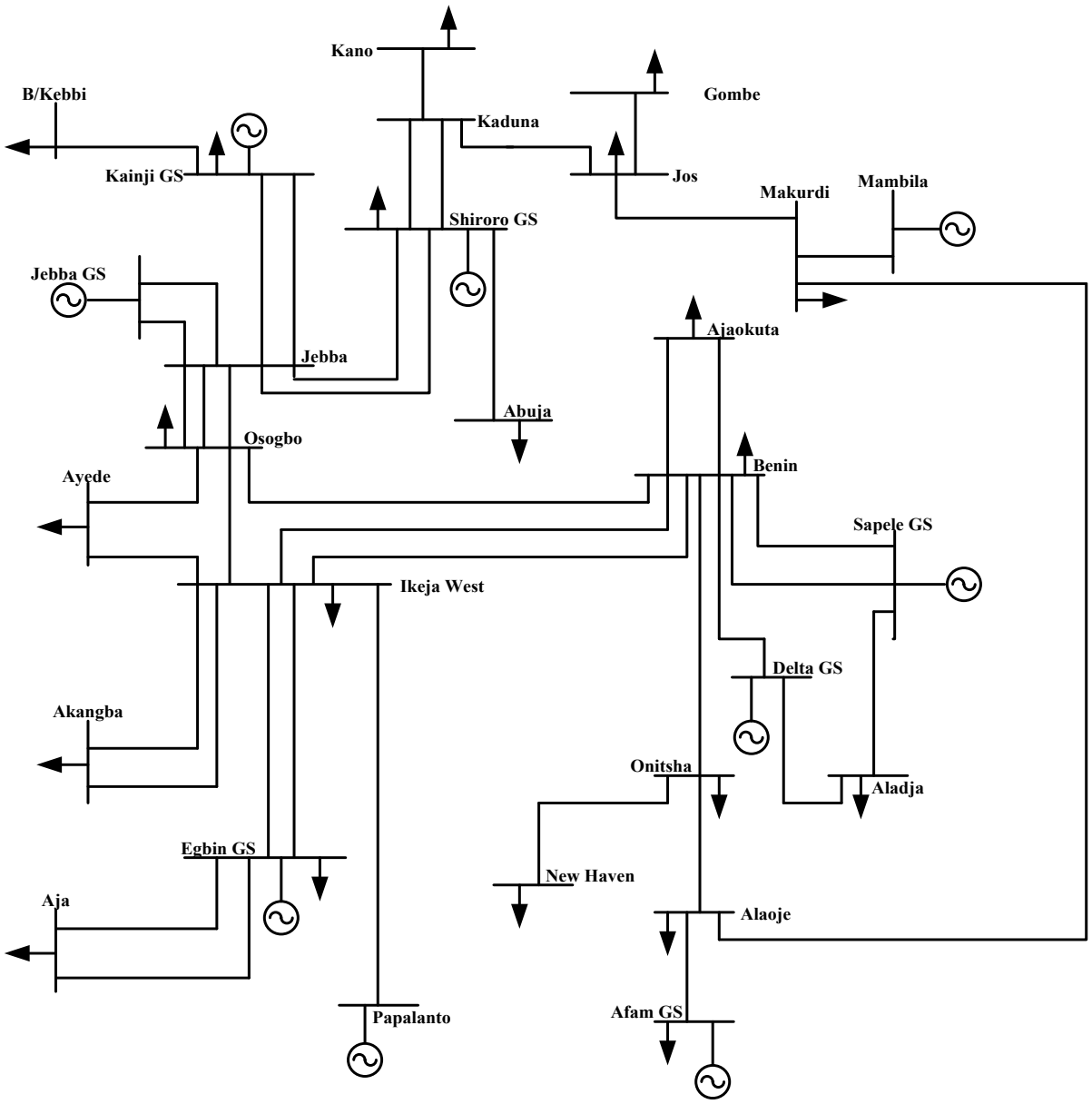

Figure 3. One-line diagram of the 28-bus model of the Nigerian 330 kV power grid [31].

Table 1. The Bus data of The Nigerian 28-bus Grid.

Bus Name	Bus Number	Bus Load, MW	Bus Load, MVAr
Egbin	1	68.90	51.70
Delta	2	0.00	0.00
Aja	3	274.40	205.80
Akangba	4	244.70	258.50
Ikeja-West	5	633.20	474.90
Ajaokuta	6	13.80	10.30
Aladja	7	96.50	72.40
Benin	8	383.30	287.50
Ayede	9	275.80	206.8
Osogbo	10	201.20	150.90
Afam	11	52.50	39.40
Alaoji	12	427.00	320.20
New-Heaven	13	177.90	133.40
Onitsha	14	184.60	138.40
B/Kebbi	15	114.50	85.90
Gombe	16	130.60	97.90
Jebba	17	11.00	8.20
Jebba G	18	0.00	0.00
Jos	19	70.30	52.70
Kaduna	20	193.00	144.70
Kanji	21	7.00	5.20
Kano	22	220.60	142.90
Shiroro	23	70.30	36.10
Sapele	24	20.60	15.40
Abuja	25	110.00	89.00
Makurdi	26	290.10	145.00
Mambila	27	0.00	0.00
Papalanto	28	0.00	0.00

Table 2. Branch Data of the Nigerian 28-Bus Grid.

Bus, (From)	Bus, (To)	Resistance, R(pu)	Reactance, X(pu)
1	3	0.0006	0.0044
4	5	0.0007	0.0050
1	5	0.0023	0.0176
5	8	0.0110	0.0828
5	9	0.0054	0.0405
5	10	0.0099	0.0745
6	8	0.0077	0.0576
2	8	0.0043	0.0317
2	7	0.0012	0.0089
7	24	0.0025	0.0186
8	14	0.0054	0.0405
8	10	0.0098	0.0742
8	24	0.0020	0.0148
9	10	0.0045	0.0340
15	21	0.0122	0.0916
10	17	0.0061	0.0461
11	12	0.0010	0.0074
12	14	0.0060	0.0455
13	14	0.0036	0.0272
16	19	0.0118	0.0887
17	18	0.0002	0.0020
17	23	0.0096	0.0271
17	21	0.0032	0.0239
19	20	0.0081	0.0609
20	22	0.0090	0.0680
20	23	0.0038	0.0284
23	25	0.0038	0.0284
12	26	0.0071	0.0532

Table 3. The Generator Data of the Nigerian 28-Bus Grid.

Identification			Generator		Reactive Limits	
Bus	Number	Voltage Mag	MW	MVAr	Qmin	Qmax
Egbin	1	1.05	0.00	0.00	-1006	1006
Delta	2	1.05	670.00	0.00	-1030	1000
Afam	11	1.05	431.00	0.00	-1000	1000
Jebba G	18	1.05	495.00	0.00	-1050	1050
Kanji	21	1.05	624.70	0.00	-1010	1010
Shiroro	23	1.05	388.90	0.00	-1010	1010
Sapele	24	1.05	190.30	0.00	-1010	1010
Mambila	27	1.05	750.00	0.00	-1010	1010
Papalanto	28	1.05	750.00	0.00	-1010	1010

Let P_{woc} and P_{wc} be the system's active power losses without and with compensation respectively while R_{woc} and R_{wc} are the annual revenue losses without and with compensation respectively.

R_{woc} and R_{wc} are related to P_{woc} and P_{wc} by equations (32) and (33) respectively:

$$R_{woc} = P_{woc} \times ₦7.49 \times 24 \times 365 \tag{30}$$

$$R_{wc} = P_{wc} \times ₦7.49 \times 24 \times 365 \tag{31}$$

The annual saving in revenue arising from the application of compensation on the Nigerian electricity grid is obtained from equations (34) and (35):

$$S_a = R_{wc} - R_{woc} \tag{32}$$

$$S_a = ₦7.45 \times 24 \times 365 \times (P_{wc} - P_{woc}) \tag{33}$$

3 Results and discussion

The Nigerian 28-bus grid without compensation as represented by the PSAT model in Figure 4 shows that Gombe, Jos, Kano, New Haven, Makurdi, Onitsha and Ayede whose voltage values were respectively 0.8353, 0.8658, 0.8712, 0.8853, 0.8897 0.9281 and 0.9333 p.u. infringed the acceptable voltage tolerance limit of 0.95 to 1.05 p.u. for stable system operation. These buses were, therefore, classified as constrained buses since they violated the statutory voltage limit of operation. The system's overall active and reactive power losses were 188.76 MW and 1,371.65 MVAr, respectively.

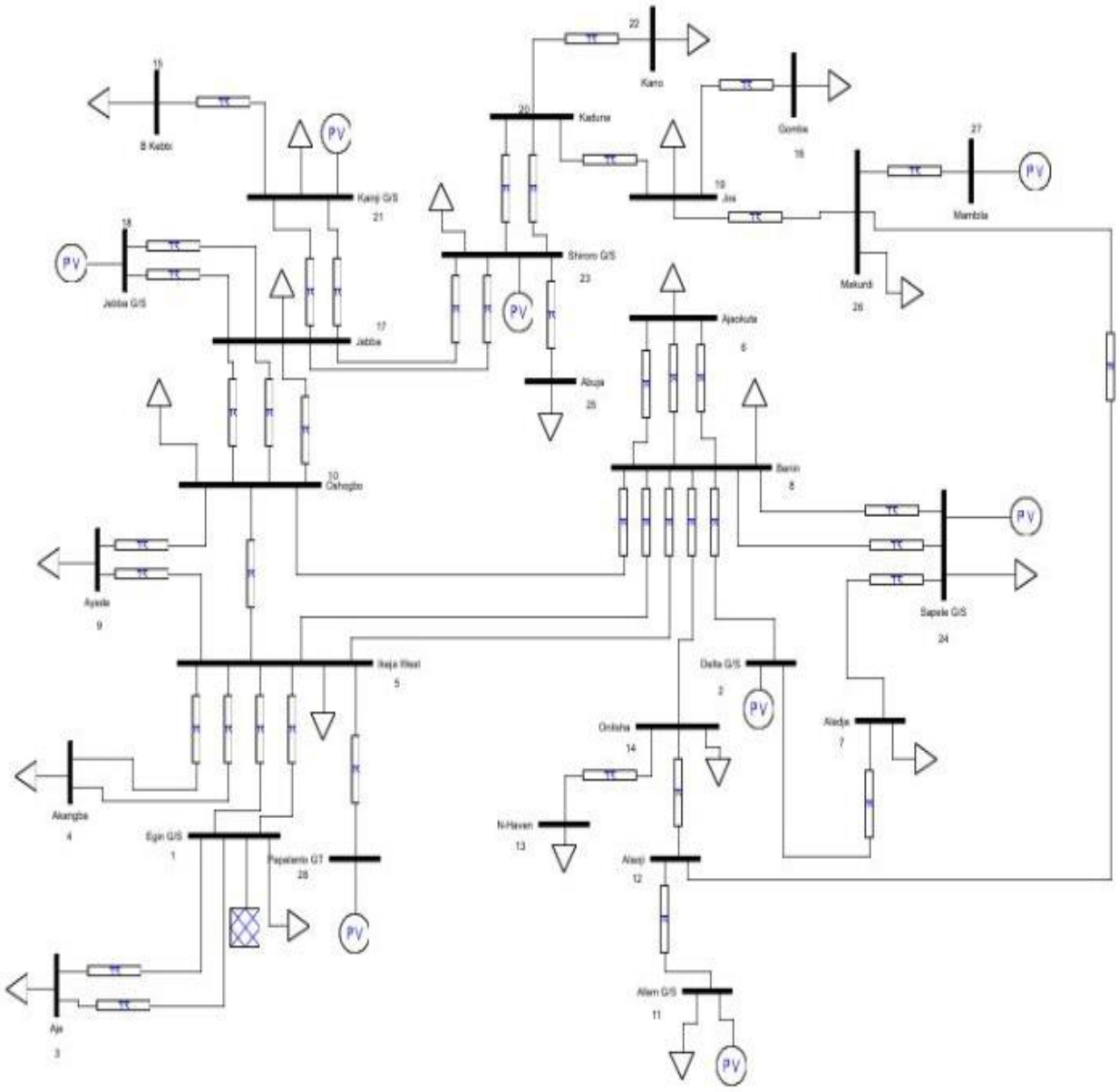

Figure 4. PSAT model of the 28-bus model of the Nigerian power grid with no FACTS device.

However, after including the combination of STATCOMs and SSSCs in the grid as shown in the PSAT model of Figure 5, the compensating devices positively impacted the voltage profile of the grid. The combined STATCOM-SSSC impacted Ayede, Birnin Kebbi, Kano and Oshogbo with respective voltage magnitudes of 0.9914, 0.9872, 0.9916 and 0.9995 p.u. Comparison of the improvement rendered by STATCOM only, SSSC only and combined STATCOM-SSSC on the overall voltage profile of the system according to Figure 6 showed that combined STATCOM-SSSC had a better impact than STATCOM only and SSSC only.

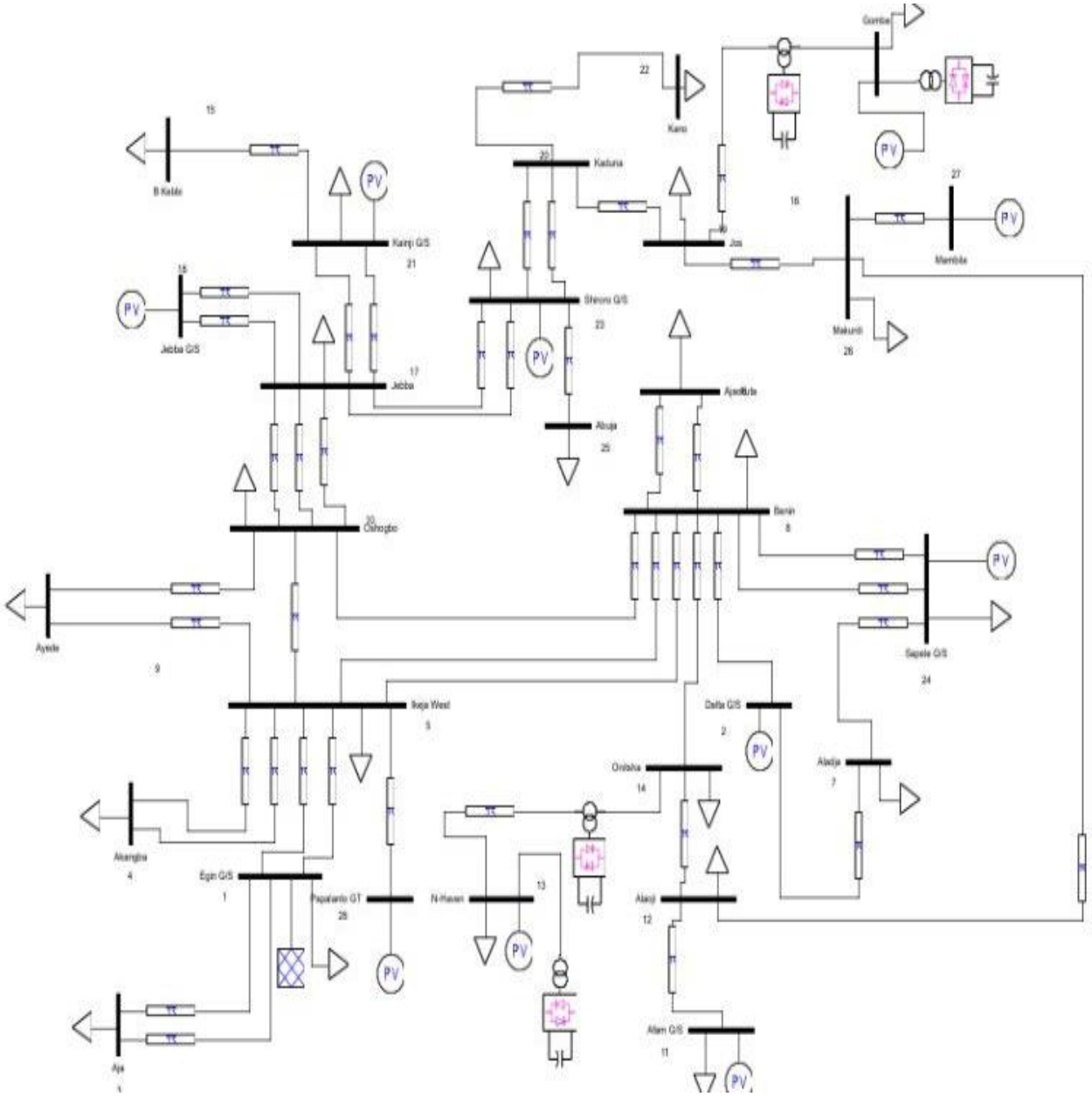

Figure 5. PSAT model of the Nigerian 28-bus grid with combined STATCOM-SSSC.

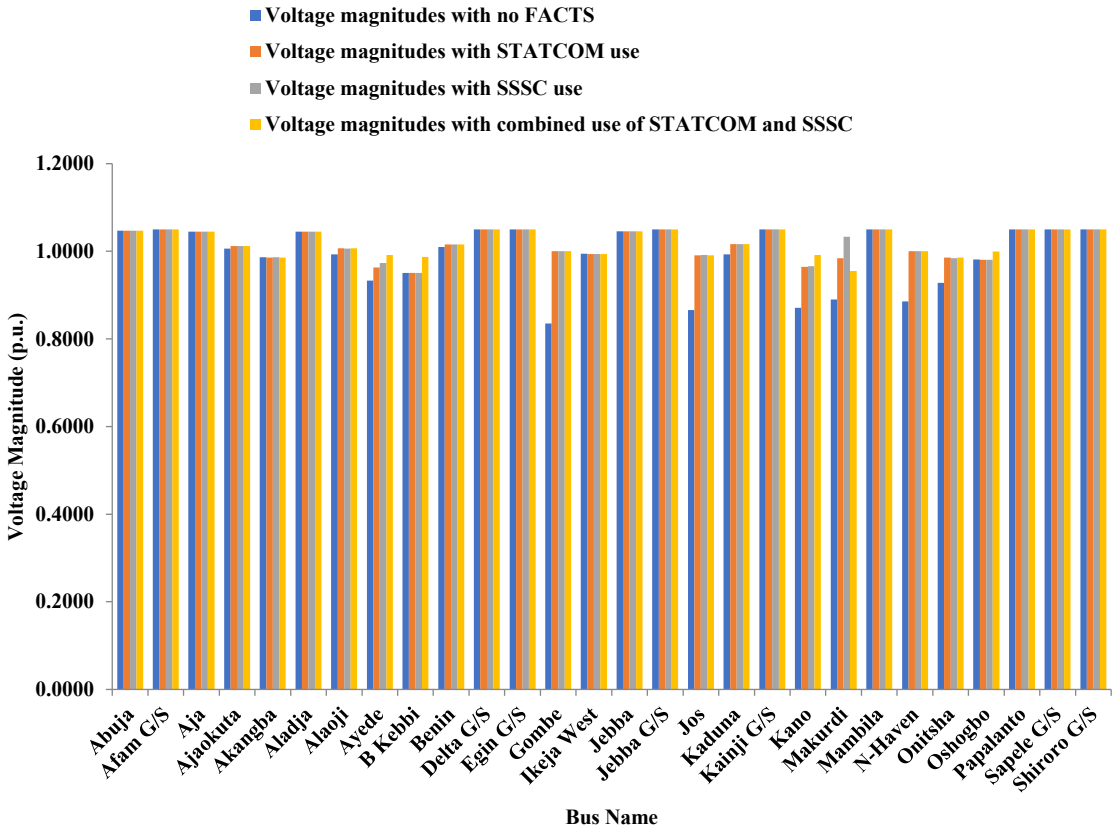

Figure 6. Comparison of the Nigerian 28-bus grid voltage profile without and with STATCOM, SSSC and combined STATCOM-SSSC.

The obtained system's overall active power losses from the STATCOM-only, SSSC-only and combined STATCOM-SSSC applications on the Nigerian 28-bus grid are presented in Figure 7. According to Figure 7, STATCOM only, SSSC only and combined STATCOM-SSSC application decreased the system's overall active power loss from 188.76 MW to 174.51, 170.21 and 165.11 MW, resulting in respective 7.55, 9.83 and 12.51% improvement in the active line flows. According to Figure 8, the overall reactive power loss of the system with the use of the three compensating devices also diminished from 1371.65 MVAr to 1288.39, 1284.91 and 1280.39 MVAr, producing an improvement of 6.07, 6.32 and 6.65% respectively in the reactive power loss. Comparison of the effectiveness of the three compensators as shown in Figures 7 and 8 revealed that the combined use of STATCOM and SSSC offered a better performance improvement over either STATCOM only or SSSC only, producing the lowest power losses of the three compensators.

The cost analysis, based on Equations 34 and 35, showed that the overall active power loss of 188.76 MW recorded when no compensating device was applied on the Nigerian 28-bus grid resulted in an annual revenue loss of ₦12,384,996,624.00. The 174.51, 170.21 and 165.11 MW overall active power losses respectively produced by STATCOM only, SSSC only and combined STATCOM-SSSC when installed on the grid reduced the annual revenue loss to ₦11,418,650,006.40, ₦11,167,886,604.00 and ₦10,833,263,364.00 respectively. These amounts showed that compensation by STATCOM only, SSSC only and combined STATCOM-SSSC generated annual cost savings of ₦934,694,584.20, ₦1,216,742,774.52 and ₦1,551,261,046.76, respectively in transmitting electrical power over the Nigerian 28-bus power grid.

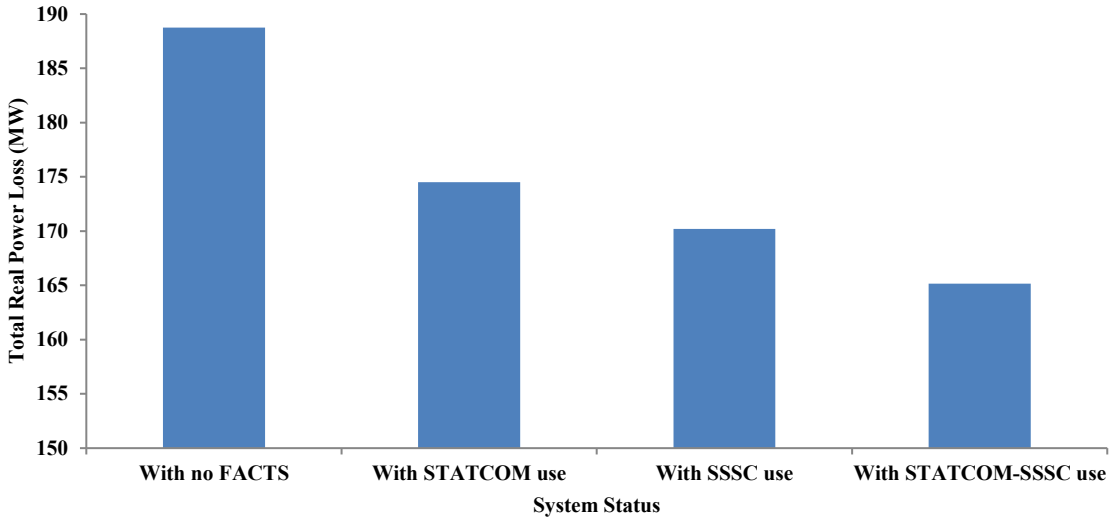

Figure 7. Comparison of the Nigerian 28-bus grid overall active power loss without and with STATCOM, SSSC and combined STATCOM-SSSC.

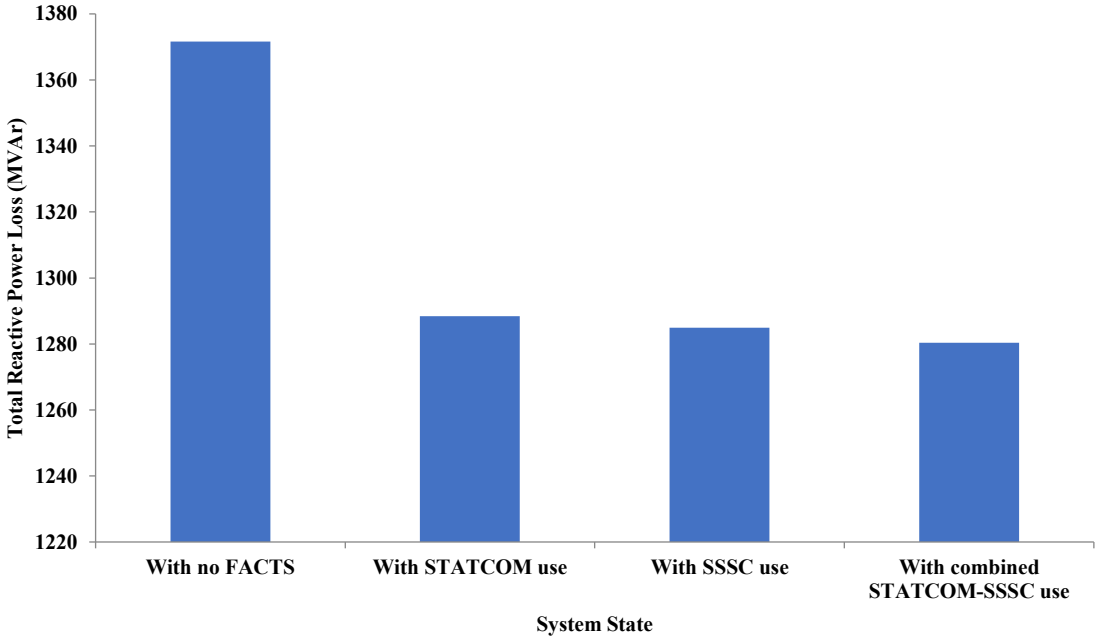

Figure 8. Comparison of the Nigerian 28-bus grid overall reactive power loss without and with STATCOM, SSSC and combined STATCOM-SSSC.

A general comparison of the effectiveness of the three compensators on the considered Nigerian electricity grid indicated that the combined use of STATCOM and SSSC exhibited a better performance improvement than either STATCOM or SSSC by producing the best overall voltage profile improvement and lowest power losses on the system with the added advantage of highest saving in revenue loss compared to the two other controllers. The findings from this study aligned with the output of the works [26][27] which are two of the very scarce literature on the combined effects of STATCOM and SSSC for improvement of voltage stability in power systems. The work of [26] identified combined STATCOM and SSSC as one of the considered hybrid controllers that exhibited superior performance over individual shunt or series controllers for voltage stability improvement. [27] through their investigation found out that combined STATCOM and SSSC showed superiority over shunt or series controllers in improving the voltage stability of a power system network. The

outcomes of the present study are consistent with these findings where combined STATCOM and SSSC showcased itself as a better compensator for power system voltage stability over STATCOM and SSSC which are respectively shunt and series compensators.

4 Conclusion

In this study, the combined effect of STATCOM and SSSC to improve voltage stability in the power system was investigated using a test case of the Nigerian 330 KV, 28-bus power grid. The steady-state response of the system was modelled using Newton-Raphson load flow equations. The simulations with STATCOM, SSSC and combined STATCOM-SSSC were carried out using MATLAB/PSAT software. The voltage profile of the system, the power losses and the cost savings in the transmission of electrical energy resulting from the use of the three controllers were determined and analysed. The results revealed that the three controllers deployed offered appropriate compensation in the considered network by improving the bus voltage magnitudes such that no violations were recorded and overall active and reactive power losses were kept to the barest minimum with appreciable savings in revenue associated with the export of electric power on the network. The combined STATCOM-SSSC, however, exhibited superiority over STATCOM and SSSC in enhancing the system voltage and line losses. The combined STATCOM-SSSC improved the bus voltage magnitudes most and produced the lowest overall active and reactive line losses with the highest savings in revenue for electric power transmission on the considered network. This study found out that STATCOM and SSSC used in combined mode offered a better performance enhancement with cost savings over STATCOM and SSSC individually deployed and therefore, are considered suitable candidate for voltage stability improvement on the Nigerian electricity grid.

References

[1] Kishore TS, Patro ER, Harish V, Haghighi AT. (2021) A comprehensive study on the recent progress and trends in development of small hydropower projects. Energies. 14(10):2882. https://doi.org/10.3390/en14102882

[2] Khubrani MM, Alam S. (2023) Blockchain-based microgrid for safe and reliable power generation and distribution: A case study of saudi arabia. Energies. 16(16):5963. https://doi.org/10.3390/en16165963

[3] Massaoudi M, Abu-Rub H, Refaat SS, Chihi I, Oueslati FS.(2021) Deep learning in smart grid technology: A review of recent advancements and future prospects. IEEE Access. 9:54558–78. https://doi.org/10.1109/ACCESS.2021.3071269

[4] Kundur P, Paserba J, Ajjarapu V, Andersson G, Bose A, Canizares C, et al. (2024) Definition and classification of power system stability IEEE/CIGRE joint task force on stability terms and definitions. IEEE Trans Power Syst. 19(3):1387–401. https://doi.org/10.1109/TPWRS.2004.825981

[5] Mokred S, Wang Y, Chen T. (2023) A novel collapse prediction index for voltage stability analysis and contingency ranking in power systems. Prot Control Mod Power Syst. 8(1):1–27. https://doi.org/10.1186/s41601-023-00279-w

[6] Peyghami S, Palensky P, Blaabjerg F. (2020) An overview on the reliability of modern power electronic based power systems. IEEE Open J Power Electron. 1:34–50. https://doi.org/10.1109/OJPEL.2020.2973926

[7] Wondie TT, Tella TG. (2022) Voltage stability assessments and their improvement using optimal placed static synchronous compensator (STATCOM). J Electr Comput Eng. 2022. https://doi.org/10.1155/2022/2071454

[8] Manohar TG, Reddy RS. (2012) Literature Review on Voltage stability phenomenon and Importance of FACTS Controllers In power system Environment. Glob J Res Eng Electr Electron Eng. 12:24–9.

[9] Ekic A, Wu D, Huang Y. A (2022) Review on Cascading Failure Analysis for Integrated Power and Gas Systems. In: 2022 IEEE 7th International Energy Conference (ENERGYCON). IEEE; 2022. p. 1–5. https://doi.org/10.1109/ENERGYCON53164.2022.9830223

[10] Hatziargyriou N, Milanovic J, Rahmann C, Ajjarapu V, Canizares C, Erlich I, et al. (2020) Definition and classification of power system stability–revisited & extended. IEEE Trans Power Syst. 36(4):3271–81. https://doi.org/10.1109/TPWRS.2020.3041774

[11] Shair J, Li H, Hu J, Xie X. (2021) Power system stability issues, classifications and research prospects in the context of high-penetration of renewables and power electronics. Renew Sustain Energy Rev. 145:111111. https://doi.org/10.1016/j.rser.2021.111111
[12] Adebisi OI, Adejumobi IA, Ogunbowale PE, Ade-Ikuesan OO. (2018) Performance Improvement of Power System Networks Using Flexible Alternating Current Transmission Systems Devices: The Nigerian 330 kV Electricity Grid as a Case Study. LAUTECH J Eng Technol. 12(2):46–55. https://laujet.com/index.php/laujet/article/view/234
[13] Adebisi OI, Adejumobi IA, Ogunbowale PE, Ade-Ikuesan OO. (2017) Application of Static Var Compensator for Voltage Stability Enhancement and Power Loss Reduction in Power System Networks.LAUTECH Journal Engineering Technology. 11(2):46–58. https://laujet.com/index.php/laujet/article/view/225
[14] Jokojeje RA, Adejumobi IA, Mustapha AO, Adebisi OI. (2015) Application of Static Synchronous Compensator (Statcom) in Improving Power System Performance: A Case Study of the Nigeria 330 kV Electricity Grid. Niger J Technol. 34(3):564–72. http://dx.doi.org/10.4314/njt.v34i3.20
[15] Marouani I, Guesmi T, Alshammari BM, Alqunun K, Alshammari AS, Albadran S, et al. (2023) Optimized FACTS devices for power system enhancement: applications and solving methods. Sustainability. 15(12):9348. https://doi.org/10.3390/su15129348
[16] Nadeem M, Imran K, Khattak A, Ulasyar A, Pal A, Zeb MZ, et al. (2020) Optimal placement, sizing and coordination of FACTS devices in transmission network using whale optimization algorithm. Energies. 13(3):753. https://doi.org/10.3390/en13030753
[17] Raj A, Vishwakarma D. Power Flow Analysis Of Synchronous Series Compensator (SSSC) in Power System.
[18] Hassan R, Shyaa SS. (2021) Simulink implementation of voltage stability improvements using STATCOM based 5-level diode clamped converter. In: IOP Conference Series: Materials Science and Engineering. IOP Publishing; 2021. p. 12009. https://doi.org/10.1088/1757-899X/1105/1/012009
[19] Ahmed I, Saurabh S, Kumar R. GA (2020) Based Optimal STATCOM Placement for Improvement of Voltage Stability. In: 2020 International Conference on Renewable Energy Integration into Smart Grids: A Multidisciplinary Approach to Technology Modelling and Simulation (ICREISG). IEEE; 2020. p. 43–8. https://doi.org/10.1109/ICREISG49226.2020.9174210
[20] Bisht K, Kumar D, Bedi KS. (2020) Enhancement of power transfer capacity and transmission efficiency using SSSC. Int J Eng Adv Technol. 9(3):2846–50.
[21] Chourasia MS, Soubache ID, Gomathi P. (2020) Voltage stability index improvement system by optimal placement of STATCOM in distributed systems. Turkish J Comput Math Educ. 11(3):1175–87.
[22] Devalkumar M, Vyas SR. (2020) Voltage Stability Improvement by using STATCOM. Int Res J Eng Technol. 7(3):4209–12.
[23] Magadum RB, Chitragar NR, Dodamani SN, Gopikrishna P V. (2020) Impact on Voltage Stability With Integration of Multiple STATCOM at Different Loading Conditions. In: 2020 5th International Conference on Devices, Circuits and Systems (ICDCS). IEEE; 2020. p. 321–5. https://doi.org/10.1109/ICDCS48716.2020.243608
[24] Opana S, Charles JK, Nabaala A. (2020) STATCOM Application for Grid Dynamic Voltage Regulation: A Kenyan Case Study. In: 2020 IEEE PES/IAS PowerAfrica. IEEE; 2020. p. 1–5. https://doi.org/10.1109/PowerAfrica49420.2020.9219888
[25] Sreedharan S, Joseph T, Joseph S, Chandran CV, Vishnu J, Das V. (2020) Power system loading margin enhancement by optimal STATCOM integration–A case study. Comput Electr Eng. 81:106521. https://doi.org/10.1016/j.compeleceng.2019.106521
[26] Mbae M, Nwulu N. (2022) Impact of hybrid FACTS devices on the stability of the Kenyan power system. Int J Electr Comput Eng. 12(1):12–21.
[27] Tiwari S, Kumar A, Sengupta S. (2018) Voltage stability analysis with a novel hybrid controller using shunt and series combination of FACTS device. In: 2018 3rd IEEE International Conference on Recent Trends in Electronics, Information & Communication Technology (RTEICT). IEEE; 2018. p. 885–90. https://doi.org/10.1109/RTEICT42901.2018.9012250

[28] Saadat H. 'Power System Analysis', Tata McGraw Hill Publishing Company, New Delhi, 2002. Bharathidasan Engineering College; 2015.
[29] Elijah OO, Iyanuoluwa OD, Oluwole OO. (2017) An Overview of Mathematical Steady-State Modelling of Newton-Raphson Load Flow Equations Incorporating LTCT, Shunt Capacitor and FACTS Devices. vol. 2017;4:3163–79.
[30] Seifi A, Gholami S, Shabanpour A. (2010) Power flow study and comparison of FACTS: Series (SSSC), Shunt (STATCOM), and Shunt-Series (UPFC). Pacific J Sci Technol. 11(1):129–37.
[31] Olabisi PO, Ayeni G. (2023) Voltage Quality Analysis on Power Transmission Networks: A Case Study of 330kV Power Transmission Networks in Nigeria. J Eng Res Rep. 25(4):42–50.